



Research article

The effect of sand quality on the bending strength and thermal distortion of chemically bonded sand cores

Gábor Gyarmati^{*}, Imre Budavári, György Fegyverneki, László Varga

Foundry Institute, University of Miskolc, 3515, Miskolc-Egyetemváros, Hungary

ARTICLE INFO

Keywords:

Casting
Sand core
Quartz sand
Chemically bonded sand
Bending strength
Hot distortion

ABSTRACT

The quality of chemically bonded sand cores used during the manufacturing process of cast components is highly dependent on the properties of the sand, which constitutes the refractory base media of the core. One of the main advantages of the application of different types of sands as molding aggregates that after casting, they can be reclaimed and can be used again during core shooting. The properties of the sand, however, could be remarkably changed during the casting and reclamation processes. This study aims to investigate the effects of the properties of the base sand on the mechanical strength and thermal distortion properties of samples made from new and thermally reclaimed silica sand. For this purpose, particle size analysis, specific surface area, and loss on ignition measurements, as well as differential thermal analysis coupled with thermogravimetry, were executed on the base sands, and the sand grains were analyzed with scanning electron microscopy and X-ray diffraction. Test pieces were made with hot box and cold box technology for bending and hot distortion tests. It was found that by the utilization of reclaimed sand, cores with higher average bending strength and lower thermal deformation can be produced. These differences can be traced back to the more advantageous granulometric properties, lower impurity content, and lower thermal expansion of thermally reclaimed sand.

1. Introduction

Sand cores are extensively used in the foundry industry to form inner cavities and holes during the manufacturing of cast components. These disposable mold parts can be considered as composites typically made from natural or, in some cases, artificial sands as aggregate filler materials whose grains are bound together by organic or inorganic binders [1, 2]. With the aid of sand cores, cavities with high complexity could be formed, which is substantial during the manufacturing of automotive components like cylinder heads and engine blocks. A good example of a sand core with complex geometry is the water jacket core (Figure 1), which is used during the casting of cylinder heads. Special attention should be paid during the making of these cores, as their mechanical properties and dimensional stability could determine the soundness of the whole casting [3, 4].

There are numerous technologies available for the making of sand cores; however, in this paper, only the ones used during our research work are considered. For comprehensive reviews of these technologies, the reader is referred to the relevant references [5, 6, 7, 8, 9, 10]. In industrial practice, sand cores are usually made by blowing the sand

mixture into a core box with the aid of compressed air, where it is cured by the chemical reaction of the components of the binder system. This chemical reaction can be triggered by heat or by the application of liquid or vapor catalysts [6, 11]. The phenolic-urethane cold box (PUCB) process is one of the most frequently used core-making technology in aluminum foundries due to its high productivity, relatively low cost, and rather good mechanical properties of the cores made with this process [3, 12]. The binder system of this technology consists of a phenolic resin and a polymeric isocyanate solution. The reaction between the components, which is triggered by tertiary amine vapor, results in the formation of solid urethane resin bridges between the sand grains, which bond the particles together [13]. The hot-box process is another widely used core-making technology that is suitable for the production of high-strength cores with high dimensional accuracy under relatively short cycle times. During this process, the sand mixture, which contains a phenolic and/or furfuryl-alcohol-based resin, is blown into a preheated core box. Due to the heat exposure, the catalyst, which is usually an aqueous ammonium nitrate or ammonium chloride solution, releases acid, which accelerates the exothermic curing reaction [2, 6, 14].

^{*} Corresponding author.

E-mail address: ontgabor@uni-miskolc.hu (G. Gyarmati).



Figure 1. Water jacket core used during the manufacturing of cylinder heads.

To ensure the fulfillment of customer expectations and to consistently produce high-quality castings, the sand cores should meet numerous requirements. The cores should have sufficient initial strength after the core shooting to withstand the loads induced by the handling and manipulation actions and should have adequate final strength (especially bending strength) during the casting process to resist the flow drag and buoyant forces caused by the liquid metal [15]. High dimensional stability and hence low thermal expansion are substantially important properties, which should be maintained until a sufficiently thick solid metal layer is solidified around the sand core [16]. After solidification, the cores should be easily removed from the castings. For this reason, the cores should possess sufficient collapsibility, which is highly dependent on the degree and rate of heat exposure and the rate of thermal decomposition of the binder [17, 18]. To avoid defects like core blows, high gas permeability, and low gas evolution are needed. The former could be ensured by proper control of the sand grain size distribution, while the latter is dependent on the quantity of binder and volatile impurities present in the sand mixture [19, 20, 21].

The mechanical properties and the dimensional stability of the sand cores are highly dependent on the characteristics of the base sand and the applied binder, as well as the parameters of the molding/core-making procedures [22, 23, 24]. In this study, the properties of the base sand are considered. The granulometric properties (grain size distribution, grain shape) have an overwhelming effect on the binder demand, the flowability of the sand mixture during core shooting, and, in this way, on the bulk density, mechanical properties, and surface characteristics of the sand cores [10, 25, 26]. Another important factor is the impurity content of the sand, as silica sands tend to contain different minerals as contaminants, such as potash, alkali feldspars, soda, which can occur in the form of separate particles or as a layer on the surface of the silica grains. These impurities can significantly lower the adhesive strength between

the binder and the sand grains, as well as they can lower the cohesive strength of the binder bridges [27, 28].

After casting, the sand grains can be reclaimed and can be used again during core shooting. For this purpose, the used residual binder material and any metallic and nonmetallic impurities should be removed from the sand mixture. This can be done with the aid of mechanical, pneumatic, thermal, or wet reclamation technologies [29, 30]. Thermal reclamation is one of the most efficient and most widely used methods of sand reclamation, in which the binder content of the mixture is burnt off in a fluidization chamber, which results in practically zero residual binder content [7]. However, the information available in the literature regarding the changes in the characteristics of the sands subjected to this treatment and the resulting changes in the quality of sand cores is rather limited. For this reason, to fill this gap of knowledge, this study aims to compare the properties of new and thermally reclaimed silica sands and to investigate the effects of the properties of the base sands on the mechanical strength and thermal distortion properties of samples made from these sands.

2. Experimental

2.1. Sand characterization

During the experiments, two different types of silica sand were used for the production of test pieces. The first is a commercially available SH32 type foundry sand imported from Slovakia, which will be labeled as “new sand” throughout the paper. The other type labeled as “reclaimed sand” was previously used in foundry production for the manufacturing of organic resin bonded sand cores with cold, warm, and hot box technologies, then it was treated in a thermal fluidized bed thermal reclamation system. The reclamation process involved the separation of dust and fines, as well as the sieving of the reclaimed aggregate. Figure 2 shows the microscopic image of the investigated sands.

For the particle size analysis of the sands, a Retsch AS 200 vibratory sieve shaker with meshes of 0 (tray), 125, 180, 250, 355, 500, and 710 μm aperture sizes was used following the sieving procedure described by the DIN ISO 3310-1 standard [31]. For the evaluation of the actual specific surface (S_{wa}) of the sand (surface area per unit weight of the material), a DISA POF type sand specific surface testing apparatus was used. During the measurement, 50 g of clay-free sand is placed in the burette of the instrument, and the volume of the sand is noted. Based on the time required for a fixed volume of air to pass through the sand sample, the actual specific surface can be evaluated by using the graph given by the producer of the apparatus (a copy of the graph is given in Ref. [32]). The average of three consecutive measurements was used for the evaluation of the specific surface of the particles of both types of sand.

The angularity of sand grains (the deviation from spherical shape) was characterized by the evaluation of the coefficient of angularity according to Eq. (1):

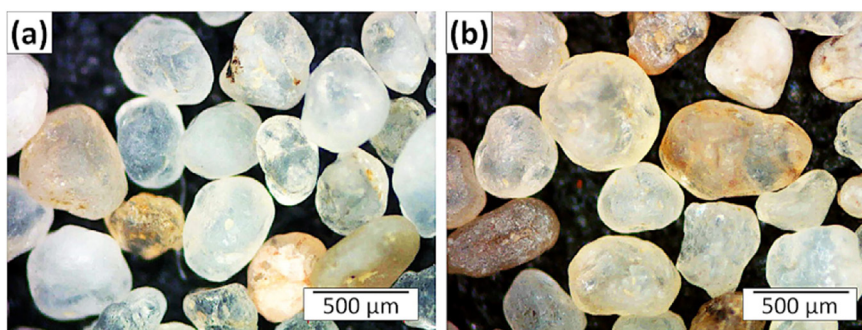


Figure 2. Microscopic image of (a) new sand and (b) reclaimed sand.

Table 1. Parameters of test piece production.

Sample type	Bending strength	Hot-distortion
Test bar dimensions [mm]	22.7 × 22.7 × 185	114.3 × 25.4 × 6.35
Technology	Polyurethane cold box (PUCB)	Hot box
Binder type	Resole phenolic resin and polyisocyanate solution	Resole phenolic resin
Catalyst	Dimethylpropylamine (vapor)	Aqueous ammonium nitrate solution
Binder content [wt. % of sand]	1.2 % (0.6 % resin and 0.6 % isocyanate)	1.5 % resin and 0.3 % catalyst
Apparatus	MULTISERW LUT	Simpson® Technologies 42109
Blowing time [s]	3	2
Blowing pressure [bar]	6	2
Tool temperature [°C]	25	220
Vapor gassing time [s]	10	-
Heating time [s]	-	20

$$E = \frac{S_{wa}}{S_{wt}} \quad (1)$$

where E is the coefficient of angularity, S_{wa} is the actual specific surface [cm^2/g] and S_{wt} is the theoretical specific surface [cm^2/g], which can be evaluated from the results of particle size analysis. For the calculation, the percentage of retained sand on each sieve must be multiplied by the appropriate theoretical surface factor, which is given by Eq. (2):

$$f = \frac{6}{d \cdot \rho} \quad (2)$$

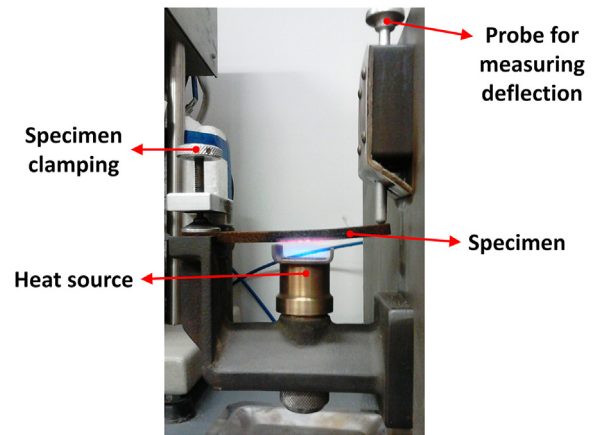
where f is the theoretical surface factor of a given sieve, d is the mean diameter of the particles retained on the sieve [cm], and ρ is the density of the material [g/cm^3]. The sum of the products of f and the percentage of retained sand divided by 100 gives the theoretical surface of the sand, assuming that each particle is perfectly spherical [33].

The moisture content of the aggregates was determined with an infrared moisture analyzer. The average of three consecutive measurements was used. The quantity of organic and other gas-forming impurities of the sands was characterized by loss on ignition (LOI) measurements. During this procedure, 2 g of the sand was heated to 900 °C in a muffle furnace for 60 min, then the percentage loss in weight was evaluated. For both types of sand, the average of three consecutive measurements was used for the characterization.

After gold sputter coating, the sand grains were inspected with a Zeiss Stemi 2000-C stereomicroscope and with a Zeiss EVO MA 10 scanning electron microscope (SEM) equipped with energy-dispersive X-ray spectroscopy (EDS) system. For the investigation of phases present in the sands, powder X-ray diffraction was utilized with a Bruker D8 Discover diffractometer (Cu K- α radiation at 40 kV accelerating voltage and 40 mA tube current) on samples weighing about 1 g prepared by grinding in a mortar. The quantification of crystalline and amorphous phases was realized by the Rietveld refinement method. The thermal properties of the sands were investigated with derivatographic measurements. The derivatograph apparatus can perform differential thermal analysis (DTA) and thermogravimetric (TG) measurements simultaneously on the same sample. For the investigations, a MOM Derivatograph-C apparatus was used with a standard platinum crucible; the rate of heating was 10 °C/min, the maximum temperature of the measurement was 1000 °C. $\alpha\text{-Al}_2\text{O}_3$ was used as reference material; the mass of each sand sample, which were prepared by grinding in a mortar, was 0.2 g. In the case of both sand types, 4 consecutive measurements were executed.

2.2. Sample preparation

Test pieces were prepared from sand-binder mixtures, which were made in 2 kg batches using a laboratory mixer. The parameters of sample preparation are given in Table 1. For the testing of the bending strength, test bars were produced with a MULTISERW LUT universal core blower

**Figure 3.** Experimental setup for hot distortion testing.

equipped with a core box for three test bars per shot. The specimens made for hot-distortion testing were produced with a Simpson® Technologies 42109 test pieces blower. The selection of the core making technique was based on the foundry practice; the PUCB process was chosen for the specimens used for bending strength evaluation as it is the most common core-making technology used in aluminum foundries [12]. The hot box process is most frequently used for the production of cores with rather thin sections [7], and as the test pieces of the hot-distortion testing are reasonably thin, to get more representative results, this process was chosen for the preparation of the specimens.

2.3. Testing methods

3-point bending tests were executed after storage times of 10 s, 35 s, 60 s, 10 min, 1 h, 6 h, and 24 h with a MULTISERW LRU-2e universal strength testing machine. The storage times were selected based on the production practice, as the measurements after 10 s, 35 s, 60 s, and 10 min give information about the strength of cores while they are manipulated and transported immediately after core shooting. The results after 1 h, 6 h, and 24 h represent the mechanical properties of the cores while they are used during the casting process. Average values and standard deviations were calculated from the results of 6 measurements.

To characterize the deformation behavior of chemically bonded sand cores when they are exposed to heat, hot-distortion tests were executed on test pieces made from new and reclaimed sands using a Simpson® Technologies Hot Distortion Tester apparatus (Figure 3). During this method, a fixed test piece is heated on one side while the deflection of the end of the specimen is measured over time. The recorded curve gives useful information about the deformation behavior and collapsibility of the sand cores made with similar technological parameters as the test

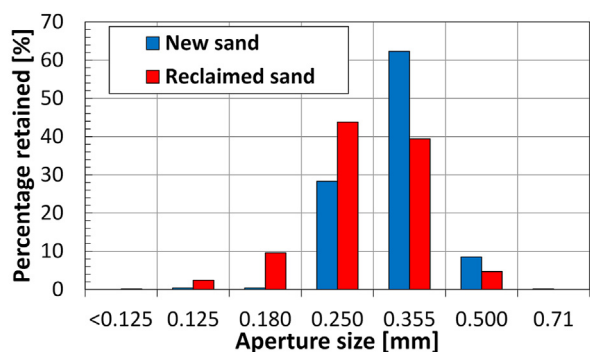


Figure 4. Grain size distribution evaluated by sieve analysis.

pieces [34]. For both types of sands, 5 specimens were tested from which average curves were evaluated.

3. Results and discussion

The results of the sieve analysis are shown in Figure 4. Table 2 summarizes the properties of the two types of sands used during the experiments. Based on Figure 4, the grain size distribution of the two sand types is a bit different. In the case of new sand, most sand grains were retained on the mesh, which has a 0.355 mm mesh size, while the main fraction of reclaimed sand grains was retained on the 0.250 mm mesh. Contrary to the new sand, reclaimed sand has a significant amount of finer particles retained on 0.180 and 0.125 mm meshes. The average grain size, as well as the grain fineness number of the reclaimed sand, is significantly lower than that of the new sand. The difference between the grain size distribution can be traced back to the different sources of the sands, as new sand was classified by the supplier of the sand, while reclaimed sand was sieved and classified by the foundry in which the thermal reclamation was realized. During thermal reclamation, due to the thermal cycling and the collision of the sand grains with each other and with the walls of the reclaimer, a notable amount of grains are

shattered, which leads to the formation of finer particles and dust, so dust separation and particle classification can be highly advantageous before the utilization of reclaimed sand [35, 36, 37]. Another possible reason for the presence of finer particles in the reclaimed sand can be that the sand grains fractured during the handling process of the sand in the foundry, which provided the reclaimed aggregate.

Reclaimed sand has a higher theoretical and actual specific surface, which is most likely the consequence of the smaller average grain size. On the other hand, reclaimed sand has a bit lower coefficient of angularity, which is probably due to the reclamation process. During the reclamation process, the sand grains are subjected to a certain degree of mechanical attrition due to the collision of the particles with each other and with the walls of the reclamation apparatus [35, 36, 37, 38].

The loss on ignition value of the new sand is more than four times higher than that of the reclaimed sand, which indicates that the new sand contains significantly more gas-forming impurities. During the microscopic examination of the sand grains, numerous stains were found on the surface of the new sand particles, which also indicates the presence of impurities (Figure 5). During the EDS-SEM analysis of the surface of the new sand grains, it was found that the stains which have a whitish color have a significantly different chemical composition than the base sand.

Figure 6 presents the results of the EDS analyses made on the surface of reclaimed (Figure 6 (a)) and new sand grains (Figure 6 (b) and (c)). During the evaluation of the elemental composition of the investigated areas, the gold content, which is the consequence of the sputter coating sample preparation, was not taken into account. In the case of the investigated reclaimed sand grain (area 1 in Figure 6 (a)), only the presence of O and Si could be detected, which indicates that the grain mainly consists of silica. The two investigated region of the new sand grain presented in Figure 6 (b) has a remarkably different chemical composition, which is even manifested by the noticeable difference in the shade of the two areas in the backscattered electron (BSD) SEM image.

In area 3 of Figure 6 (b), only Si, O, and a minimal amount of Al could be detected, which suggests that the analyzed region mostly consists of silica. Area 2 of Figure 6 (b), however, contains high quantities of Al, K, and a small amount of Na. The new sand grain shown in Figure 6 (c) contains a significant amount of Al, K, and minor quantities of Na and Fe

Table 2. Results of sand characterization.

Sand type	New sand	Reclaimed sand
Average grain size [μm]	403.3	351.1
AFS grain fineness number	33.95	40.84
Actual specific surface [cm^2/g]	77	84
Theoretical specific surface [cm^2/g]	58.29	69.32
Coefficient of angularity	1.32	1.21
Humidity [%]	0.037 ± 0.005	0.033 ± 0.005
Loss on ignition [%]	0.2763 ± 0.0328	0.0640 ± 0.0147

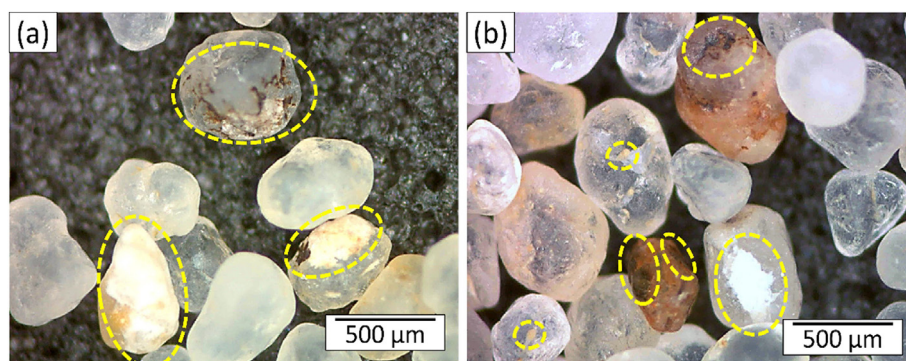


Figure 5. (a) and (b) Possible impurities on the surface of the grains of new sand.

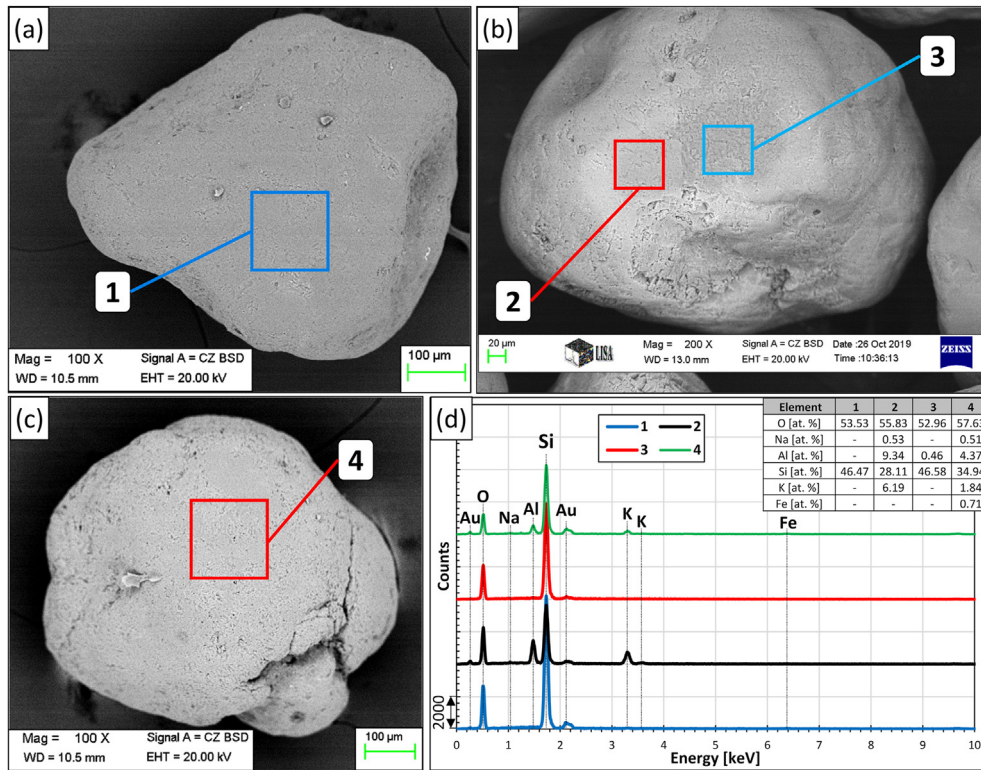


Figure 6. Backscattered electron SEM images of (a) reclaimed and (b),(c) new sand grains, (d) results of the EDS analyses of the indicated areas.

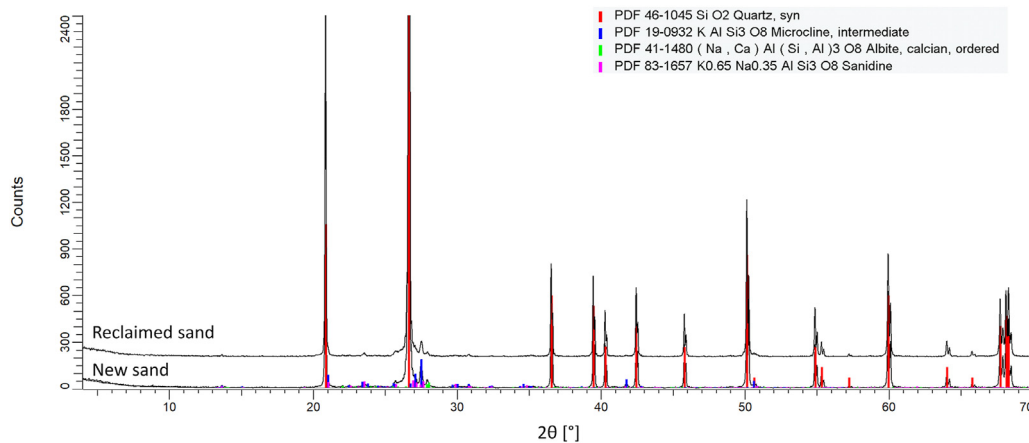


Figure 7. XRD patterns of the investigated sands.

Table 3. Results of quantitative mineralogical analysis.

Phase	New sand	Reclaimed sand
α-quartz [wt. %]	90.2	91.7
Albite [wt. %]	0.9	0.6
Microcline [wt. %]	4.1	3.2
Amorphous [wt. %]	4.8	4.5

are also present. These elements are typically present in sands in the form of oxides. These oxides are undesirable impurities of the foundry sands, as they have a negative impact on the strength properties of binder systems that utilize acid catalysts, as they tend to react with acids [39]. Besides that, Na, K, and Al are usually present in the form of porous alkali feldspars and mica, which typically have lower mechanical strength than

the silica sand and provide lower adhesive strength between the sand grains and binder bridges [27].

For a better understanding of the phases present in the sands, XRD analysis was implemented. The XRD patterns of the two aggregates are presented in Figure 7. Based on the analysis, the main constituents of both types of sand are α-quartz, microcline, albite, and the presence of trace quantities of sanidine is also possible. The results of the phase quantification (Table 3) suggest that the total content of impurity minerals besides quartz is similar in both sands; however, the reclaimed aggregate contains slightly less amount of feldspars and amorphous materials.

The minor difference between the impurity and amorphous content of the sands can be related to the thermal reclamation method. Due to the thermal cycling and the collision of the sand grains with each other and with the walls of the reclaimer, the impurities present on the grain surface can be removed due to the mechanical attrition and stresses induced

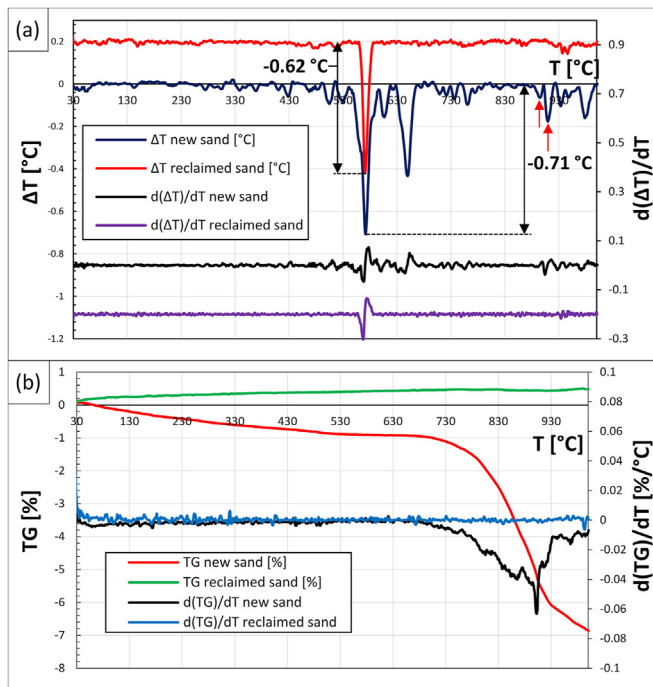


Figure 8. Results of the (a) DTA and (b) TG analyses of sand samples.

by the thermal loading. The minor difference between the amorphous content is possibly due to the recrystallization of amorphous silica and nanocrystalline quartz present in the sands at the temperatures of thermal reclamation (typically between 700 and 800 °C [29]); however, this hypothesis needs to be further investigated in the future [40, 41]. It must be highlighted that although the total content of impurity minerals is similar in both aggregates (according to the XRD analysis), based on the microscopic and SEM investigations, the quantity of impurities present on the grain surfaces is rather different; the reclaimed sand samples contain a negligible amount of impurities present in the form of stains on the grain surface (similar to the ones presented in Figure 5). This difference is crucial, as the presence of surface impurities can significantly alter the adhesive strength of the sand grain/binder bonds [28].

Figure 8 presents representative curves recorded during the DTA (Figure 8 (a)) and TG (Figure 8 (b)) analyses of the investigated sand samples. In the figure, TG represents the percentage of mass loss as a function of temperature. The derivatives of the investigated parameters with respect to the temperature are also presented to visualize the rate of temperature change (Figure 8 (a)) and the rate of mass change (Figure 8 (b)). On the DTA curve of the thermally reclaimed sand (Figure 8 (a)), only one significant endotherm peak could be detected, which indicates the polymorphic transformation of α -quartz to β -quartz at around 573 °C [42, 43]. It is reported [42] that β -quartz transforms into α -tridymite at around 870 °C. However, this transformation is highly dependent on the purity of the investigated quartz samples. Heaney [44] reported that during the heating of pure quartz, the transformation to tridymite is bypassed, and quartz directly transforms into cristobalite at ~ 1050 °C, while tridymite can be synthesized only with the aid of mineralizing agents. According to Holmquist [45], the conversion of quartz to tridymite can take place in the presence of solid or liquid alkali silicates by the solution of alkali oxides in the silica structure. He found that when quartz samples with 2 % alkali oxide content are heated, tridymite forms between 872 and 898 °C with Na_2O , as well as 883 and 902 °C with K_2O . The formation of cristobalite was also evinced above 898 °C with Na_2O and above 902 °C with K_2O . In the temperature range of 872–902 °C there are no clearly visible peaks on the DTA curve of the reclaimed sand, which indicates that the tridymite formation has not taken place during the investigation. On the other hand, in the case of new sand, there is an

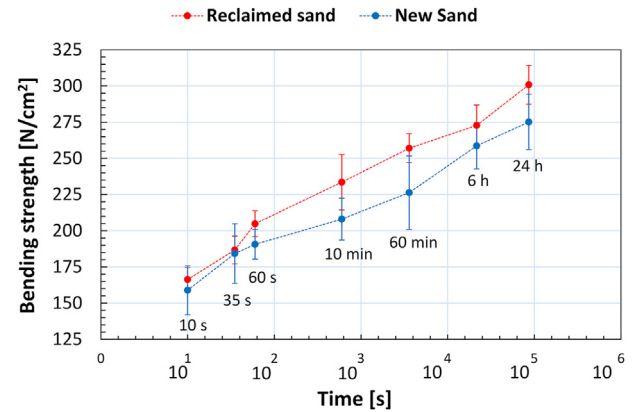


Figure 9. Results of the bending strength evaluation.

endotherm peak at 895 °C followed by a larger peak at 909 °C (indicated by red arrows in Figure 7 (a)), which could indicate the formation of tridymite around 900 °C. The peaks at temperatures higher than 930 °C can even indicate cristobalite formation [46].

In the case of foundry sands, tridymite promoting agents could be the impurities of the sands as well as engineered sand additives (ESA) and even sodium in the form of bentonite in the case of green sands [43]. Dapiaggi et al. [47] reported that in the case of ceramic mixtures containing Na- and K-bearing mineraliser compounds besides quartz, the transformation into high-temperature silica polymorphs takes place at considerably lower temperatures than in the case of pure quartz. As can be seen in Figure 8 (a), there are numerous endotherm peaks on the DTA curve of the new sand. Based on the results in Figure 6, new sand contains a significant amount of Na- and K-bearing impurities on its surface. Besides that, the XRD analysis indicates that both sands contain alkali feldspars which can act as mineralisers and can promote tridymite formation at lower temperatures. On the other hand, the fact that the high-temperature DTA peaks, which should indicate tridymite formation, are only present in the case of new sand suggests that the quantity of mineralisers is significantly higher in the new sand. However, this phenomenon clearly needs clarifying research in the future. The high number of endotherm peaks besides the peak referring to the α -quartz to β -quartz transformation indicates that the impurity content of the investigated new sand samples is quite high. This is supported by the relatively high mass loss indicated by the TG curve of new sand (Figure 8 (b)). While the mass of the reclaimed sand sample was constant during heating, the mass of the new sand was slightly decreasing until around 700 °C, when the intensity of mass loss started to increase remarkably. In the case of new sand, at around 900 °C, there is a local minimum of the derivative of the TG curve, which is accompanied by an endotherm peak on the DTA curve. This indicates the thermal decomposition of a compound present in the new sand, which is assuredly a gas-forming impurity of the sand.

The results of the bending tests made with samples produced with different base sands are presented in Figure 9.

The results indicate that the specimens made with reclaimed sand possess higher average bending strength than the ones produced from new sand. The difference between the bending strength results is significantly high, more than 10 % in the case of specimens tested after 10 and 60 min. The results might be considered somewhat unexpected since, based only on the specific surface results, the reclaimed sand should have higher binder demand. On the other hand, the grains of the reclaimed sand have a wider size distribution and a lower coefficient of angularity, which usually contributes to better flowability during core shooting and higher packing density, which can result in better mechanical properties [10]. Another reason for the difference between the bending strength results could be the difference between the impurity content of the sands. Based on the results of DTA, TG, and LOI

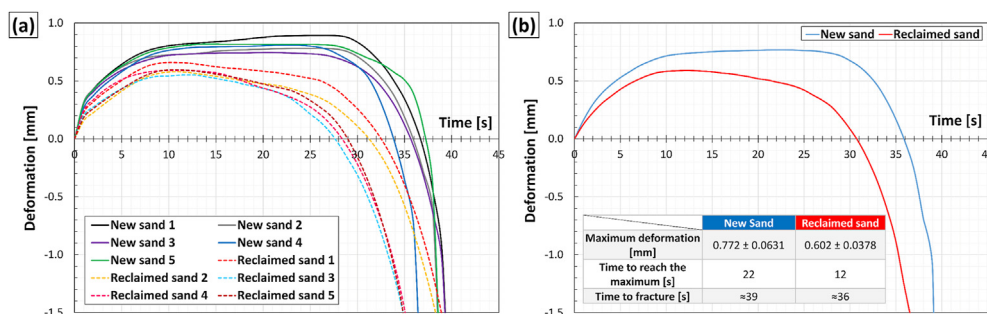


Figure 10. Results of the hot distortion tests: (a) individual measurements and (b) average curves.

measurement and SEM investigations coupled with EDS analysis, new sand contains a notable amount of contaminations on the surface of its grains, which can result in lower adhesive strength between the sand particles and binder bridges [28]. The results are consistent with the findings of *Wesp and Engelhardt* [37], who reported that for two different grades of silica sand, higher bending strength could be achieved by using thermally reconditioned sand instead of “fresh sand”.

The results of the hot distortion testing are presented in Figure 10: Figure 10. (a) shows the hot distortion curves of the individual test pieces (the hot distortion curves of individual specimens are marked as New sand 1–5 and Reclaimed sand 1–5), while the average curves and the average characteristic parameters of the curves are given in Figure 10. (b). Based on the curves, the thermal deformation characteristics of the samples made from the two types of sands are remarkably different. The maximum deformation values and the time needed to reach the maximum are notably higher when new sand is used. Excessive deformation of sand cores and molds during the casting process could lead to dimensional inaccuracies, so from this point of view, the higher deformation values are disadvantageous. The difference between the average maximum deformation values is more than 20 %, which could have serious consequences when near net-shaped castings are produced, and strict dimensional requirements should be met. As the upward deflection section of the hot distortion curves is highly influenced by the properties of the base sands [34], this noteworthy difference between the maximum deformations can be traced back to the thermal properties of the sands. Reclaimed sand, as it is subjected to temperatures higher than 573 °C during the thermal reclamation process, has undergone a phase transformation (α -quartz to β -quartz) previously. This induces semi-permanent changes in the crystal structure of the sand, which in turn becomes thermally more stable, and its thermal expansion is lowered [35, 48]. It is also noteworthy to mention that the shape of the curves also differs to some degree. In the case of new sand, after the initial relatively fast upward deflection, further positive deformation takes place at a significantly slower rate until the maximum deformation is reached. When reclaimed sand is used, the maximum deformation is immediately reached after the initial upward deflection and followed by a slow negative deformation, which transfers into the steep depression of the deformation values indicating the degradation and mechanical failure of the specimens. The time needed for the fracture of the specimens is a bit lower in the case of reclaimed sand, which indicates that the collapsibility of the sand cores made from this type of sand is higher. The maximum deformation values suggest that dimensionally more accurate cavities could be created with sand cores produced from reclaimed sand. However, in the tested time range, the time of thermal resistance is higher in the case of new sand, which could be more advantageous in the case of castings with longer solidification times [49, 50]. The reason for the differences in terms of thermal stability clearly needs to be investigated in the future.

Based on the results of hot distortion and bending tests, sand cores and molds made with reclaimed sand possess more advantageous properties (i.e., higher bending strength and lower thermal deformation). Besides that, it is important to highlight that the application of sand reclamation systems has economic and environmental benefits, as

it reduces the quantity of spent molding mixtures needed to be land-filled [29, 51].

4. Conclusion

Based on the results of this study, the following conclusions could be drawn:

- The specimens produced from reclaimed sand possess higher average bending strength than the ones produced from new sand. This is due to the differences in the granulometric properties and impurity content of the base sands.
- The results of LOI, DTA, and TG measurements, as well as the SEM investigations, indicate that new sand contains a significant amount of contaminations on the surface of its grains. Based on the XRD analysis, these contaminations contain alkali feldspars, which are present in both sands, however, the microscopic and SEM investigations revealed that the quantity of the contaminants on the grain surfaces is higher in new sand.
- Based on the hot distortion tests, the thermal deformation of sand cores made from reclaimed sand is lower. On the other hand, the thermal stability of cores made from new sand is better, which can result in lower collapsibility.

Declarations

Author contribution statement

Gábor Gyarmati: Performed the experiments; Analyzed and interpreted the data; Wrote the paper.

Imre Budavári: Conceived and designed the experiments; Analyzed and interpreted the data.

György Fegyverneki: Contributed reagents, materials, analysis tools or data.

László Varga: Conceived and designed the experiments.

Funding statement

This research did not receive any specific grant from funding agencies in the public, commercial, or not-for-profit sectors.

Data availability statement

Data will be made available on request.

Declaration of interests statement

The authors declare no conflict of interest.

Additional information

No additional information is available for this paper.

Acknowledgements

The authors thank Árpád Kovács for his assistance in the making of SEM images and EDS analysis and Tibor Ferenczi for the realization of derivatographic measurements.

References

- [1] F. Czerwinski, M. Mir, W. Kasprzak, Application of cores and binders in metalcasting, *Int. J. Cast Met. Res.* 28 (2015) 129–139.
- [2] D.M. Trinowski, Foundry, in: L. Pilato (Ed.), *Phenolic Resins A Century Prog.*, Springer-Verlag Berlin Heidelberg, 2010, pp. 451–502.
- [3] R. González, R. Colas, A. Velasco, S. Valtierra, Characteristics of phenolic-urethane cold box sand cores for aluminum casting, *Int. J. Met.* 5 (2011) 41–48.
- [4] E. Köhler, C. Klimesch, S. Bechtle, S. Stanchev, Cylinder head production with gravity die casting, *MTZ World.* 71 (2010) 38–41.
- [5] J. Jorstad, M.B. Krusiak, J.O. Serra, V. La Fay, Aggregates and binders for expendable molds, in: *ASM Handbook 15*, ASM International, 2008, pp. 528–548.
- [6] M. Holtzer, A. Kmita, *Mold and Core Sands in Metalcasting: Chemistry and Ecology Sustainable Development*, Springer Nature Switzerland AG, 2020.
- [7] J. Campbell, Molding, in: J. Campbell (Ed.), *Compleat. Cast. Handb.*, Elsevier Ltd., 2011, pp. 911–938.
- [8] M. Holtzer, R. Daňko, Molds and cores system in foundry, in: M. Holtzer, M. Górný, R. Daňko (Eds.), *Microstruct. Prop. Ductile Iron Compact. Graph. Iron Cast.*, SpringerBriefs in Materials, 2015, pp. 27–43.
- [9] H.J. Langer, W.R. Dunnavant, Foundry resins, in: *Encycl. Of Polymer Sci. Technol.*, John Wiley & Sons, Inc., 2011.
- [10] J.R. Brown, Sands and sand bonding systems, in: J.R. Brown (Ed.), *Fosco Non-ferrous Foundryman's Handb.*, Elsevier Ltd., 1999, pp. 149–166.
- [11] J. Ge, C.A. Monroe, M. Velazquez Blandino, D. Reich, The effect of coefficient of restitution in modeling of sand granular flow for core making: Part II laboratory and industrial test, *Int. J. Met.* 13 (2019) 768–782.
- [12] J. Archibald, J. Kroker, High efficiency cold box processes - technology focused on business goals, *Int. J. Met.* 7 (2013) 51–59.
- [13] F. Iden, U. Pohlmann, W. Tilch, H.J. Wojtas, Strukturen von Cold-Box-Bindersystemen und die Möglichkeit ihrer Veränderung, *Giesserei-Rundschau* 58 (2011) 3–8.
- [14] C. Macho, C. Psimenos, Angelos, G. Eder, Heiðhárðent Harze nach dem Warm- und Hot-Box-Verfahren - anforderungen des Marktes und aktuelle Entwicklungen der Fa. Furtenbach GmbH, *Giesserei-Rundschau* 54 (2007) 2–11.
- [15] B.J. Stauder, H. Kerber, P. Schumacher, Foundry sand core property assessment by 3-point bending test evaluation, *J. Mater. Process. Technol.* 237 (2016) 188–196.
- [16] J. Campbell, The concept of net shape for castings, *Mater. Des.* 21 (2000) 373–380.
- [17] H. Bargaoui, F. Azzouz, D. Thibault, G. Cailletaud, Thermomechanical behavior of resin bonded foundry sand cores during casting, *J. Mater. Process. Technol.* 246 (2017) 30–41.
- [18] B.J. Stauder, H. Harmuth, P. Schumacher, De-agglomeration rate of silicate bonded sand cores during core removal, *J. Mater. Process. Technol.* 252 (2018) 652–658.
- [19] L. Mádi, L. Varga, The effect of gas permeability on the pressure of artificial resin-bonded core gases, *IOP Conf. Ser. Mater. Sci. Eng.* 426 (2018), 012033.
- [20] H. Hudák, L. Varga, Examination of correlation between the granulometric properties of molding and core sand mixtures and their production parameters, *IOP Conf. Ser. Mater. Sci. Eng.* 903 (2020), 012060.
- [21] H. Hudák, L. Varga, Effect of the changes in bulk density and granulometric properties on the strength properties of the moulding sand mixtures, *Int. J. Eng. Manag. Sci.* 5 (2020) 116–122.
- [22] L. Mádi, L. Varga, T. Mikó, Examination of the properties of resin bonded core mixtures, *Mater. Sci. Forum* 885 (2017) 171–177.
- [23] H. Khandelwal, B. Ravi, Effect of molding parameters on chemically bonded sand mold properties, *J. Manuf. Process.* 22 (2016) 127–133.
- [24] H. Khandelwal, B. Ravi, Effect of binder composition on the shrinkage of chemically bonded sand cores, *Mater. Manuf. Process.* 30 (2015) 1465–1470.
- [25] S.M. Dobosz, A. Grabarczyk, K. Major-Gabryła, J. Jakubski, Influence of quartz sand quality on bending strength and thermal deformation of moulding sands with synthetic binders, *Arch. Foundry Eng.* 15 (2015) 9–12.
- [26] I. Vasková, L. Varga, I. Prass, V. Dargai, M. Conev, M. Hrubovčáková, M. Bartošová, B. Bulko, P. Demeter, Examination of behavior from selected foundry sands with alkali silicate-based inorganic binders, *Metals* 10 (2020) 1–16.
- [27] *Molding Methods and Materials*. Des Plaines, American Foundrymen's Society, Illinois, 1962.
- [28] V.L. Weddington, C.E. Moblely, Influence of sand surface chemistry on bonding, *AFS Trans.* 99 (1991) 825–870.
- [29] R. Daňko, Reclamation of used molding sands, in: M. Holtzer, et al. (Eds.), *Microstruct. Prop. Ductile Iron Compact. Graph. Iron Cast.*, SpringerBriefs in Materials, 2015, pp. 59–75.
- [30] J. Daňko, M. Holtzer, R. Danko, Factors influencing selection of effective reclamation techniques and assessment methods of the reclaimed material quality, *Arch. Foundry Eng.* 7 (2007) 29–32.
- [31] ISO, 3310-1:2016-08 2016-08 (E) Test Sieves – Technical Requirements and Testing – Part 1: Test Sieves of Metal Wire Cloth Standard, 2016.
- [32] *Foundry sand testing equipment operating instructions*, Ridsdale & Co Ltd, 2020. https://www.basrid.co.uk/ridsdale/images/pdf/AFS_OIM.pdf. (Accessed 28 December 2020).
- [33] A.D. Sarkar, *Mould & Core Material for the Steel Foundry*, Pergamon Press Ltd., 1967.
- [34] S. McIntyre, S.M. Strobl, Adapting hot distortion curves to process control, *Foundry Manag. Technol.* 126 (1998) 22–26.
- [35] A. Ghosh, Modern sand Reclamation technologies for economy, environment friendliness and energy efficiency, in: *Trans. 61st Indian Foundry Congr.* 2013, pp. 1–5, 2013.
- [36] M.M. Khan, S.M. Mahajani, G.N. Jadhav, R. Vishwakarma, V. Malgaonkar, S. Mandre, Mechanical and thermal methods for reclamation of waste foundry sand, *J. Environ. Manag.* 279 (2021) 111628.
- [37] S. Wesp, W. Engelhardt, Thermal reconditioning of core sand in aluminum foundry: a contribution to environmental protection, *AFS Trans.* 99 (1991) 227–235.
- [38] D.S. Leidel, Myths, misconceptions, and mistakes in sand reclamation, *AFS Trans.* 96 (1988) 21–26.
- [39] J.D. Beadle, *Castings*, The Macmillan Press Ltd., 1971.
- [40] F. Kristály, B. Török, The role of SiO₂ and silica-rich amorphous materials in understanding the origin of uncommon archeological finds, *Mater. Manuf. Process.* 35 (13) (2020) 1410–1419.
- [41] F. Kristály, Z.H. Tóth, Á. Ringer, B. Török, Archaeometry of fire aided limnosilicite mining in the Avas-Tüzköves (Miskolc, NE-Hungary) Paleolithic silica source, *Mater. Manuf. Process.* 35 (13) (2020) 1403–1409.
- [42] M. Hrubovčáková, I. Vasková, M. Benková, M. Conev, Opening material as the possibility of elimination veining in foundries, *Arch. Foundry Eng.* 16 (2016) 157–161.
- [43] J. Thiel, Thermal expansion of chemically bonded silica sands, *AFS Trans.* 119 (2011).
- [44] P.J. Heaney, Structure and chemistry of the low-pressure silica polymorphs, *Rev. Mineral. Geochem.* 29 (1994).
- [45] S.B. Holmquist, Conversion of quartz to tridymite, *J. Am. Ceram. Soc.* 44 (2) (1961) 82–86.
- [46] A. Aras, F. Kristály, α -Cristobalite formation in ceramic tile and sewage pipe bodies derived from Westerwald ball clay and its effect on elastic-properties, *Appl. Clay Sci.* 178 (2019) 105126.
- [47] M. Dapiaggi, L. Pagliari, A. Pavese, L. Sciascia, M. Merli, F. Francescon, The formation of silica high temperature polymorphs from quartz: influence of grain size and mineralising agents, *J. Eur. Ceram. Soc.* 35 (2015) 4547–4555.
- [48] E.C. Silva, I. Masiero, W.L. Guesser, Comparing sands from different reclamation processes for use in the core room of cylinder heads and cylinder blocks production, *Int. J. Met.* 14 (2020) 706–716.
- [49] M.J. Keil, J. Rodriguez, S.N. Ramrattan, Thermal distortion of shell and nobake binder systems, *AFS Trans.* 154 (1999) 71–74.
- [50] S.N. Ramrattan, S. Vellanki, O. Jideaku, C. Huang, Thermal distortion in process control of chemically-bonded sands, *AFS Trans.* 152 (1997) 161–164.
- [51] M. Dereń, M. Łuczak, A. Roczniak, A. Kmita, Influence of reclamation process on the ecological quality of reclaim sand, *Arch. Foundry Eng.* 17 (2017) 43–46.